[Ann. Tokyo Astron. Obs. 5, 73 (1957)], who included more recent observations from 1927 and 1928 as well as data from the U.S. Naval Observatory between 1938 and 1947. He gives $(6.59 \pm 0.15) \times 10^{-8}$ and $(1.095 \pm 0.022) \times 10^{-6}$, respectively, where we have converted his probable errors to standard errors. For comparison with the mass, we use 5.684×10^{26} kg for Saturn.
13. G. F. Lindal, *Bull. Am. Astron. Soc.* **13**, 700 (1981).
14. Values of radii from the Voyager imaging team are as given in B. A. Smith *et al.*, *Science* **215**, 504 (1982).
15. G. W. Null, *Astron. J.* **81**, 1153 (1976).
16. Y. Kozai, *Publ. Astron. Soc. Jpn.* **28**, 675 (1976).
17. A. J. R. Prentice, *J. Astron. Soc. Victoria* **28**, 47 (1981); *Bull. Am. Astron. Soc.* **13**, 743 (1981); in *The Origin of the Solar System*, S. F. Dermott, Ed. (Wiley, London, 1978), pp. 111–162; ____ and D. ter Haar, *Nature (London)* **280**, 300 (1979).
18. On the average, the orbital motions of Mimas and Tethys are in a 4:2 commensurability ratio with respect to a uniformly rotating axis midway between their ascending nodes on the equator of Saturn. The theory of the forced libration about this resonance state was outlined by F. Tisserand [*Theorie de Mécanique Céleste* **4**, 98 (1896)] and is discussed in more modern terms by L. Blitzer and J. D. Anderson (*Celest. Mech.*, in press). General reviews of orbit-orbit resonances in the solar system have been given by S. J. Peale [*Annu. Rev. Astron. Astrophys.* **14**, 215 (1976)] and R. Greenberg [in *Planetary Satellites*, J. A. Burns, Ed. (Univ. of Arizona Press, Tucson 1977); *Vistas Astron.* **21**, 209 (1977)].
19. A. J. R. Prentice, private communication. A simplified numerical code was used to determine the effects of compression by assuming the satellites to be chemically undifferentiated and using the data of M. J. Lupo and J. S. Lewis [*Icarus* **40**, 157 (1979)] for the compressibility of rock and ices. Water, ammonia, and methane ices were considered. A methane clathrate was also included in a model but was found not to define a distinctive class by density because of its low abundance.
20. J. S. Lewis, *Icarus* **16**, 241 (1972); *Science* **186**, 440 (1974).
21. J. E. Ross and L. H. Aller, *Science* **191**, 1223 (1976).
22. L. A. Lebofsky, *Icarus* **25**, 205 (1975).
23. Y. Kozai (*16*) determined the mass of Dione as $(1.85 \pm 0.04) \times 10^{-6}$ times the mass of Saturn by using the theory of M. Rapaport [*Astron. Astrophys.* **22**, 179 (1973)] for the forced eccentricity.
24. We thank the members of the Voyager Project operations team and the Deep Space Network for their support in the acquisition of the radio science data. We thank the Voyager navigation team for their help in preparing data files for the celestial mechanics phase of the investigation, for making their software available to us, and for giving us the benefit of their experience in fitting orbits to radio and optical navigation data. We particularly acknowledge the direct involvement of J. K. Campbell in the determination of masses for Tethys and Iapetus. We thank the Voyager imaging team for prepublication values of radii. We also thank A. J. R. Prentice for numerous discussions and assistance in calculations, plus prepublication results on model satellite densities. We especially thank B. J. Buckles, P. E. Doms, D. F. Finnerty, and D. P. Holmes for their help in the implementation and execution of these experiments, and H. B. Hotz and D. N. Sweetnam for their help in the occultation profile reduction. This work was supported by the National Aeronautics and Space Administration.

10 November 1981; revised 23 November 1981

Magnetic Field Studies by Voyager 2: Preliminary Results at Saturn

Abstract. *Further studies of the Saturnian magnetosphere and planetary magnetic field by Voyager 2 have substantiated the earlier results derived from Voyager 1 observations in 1980. The magnetic field is primarily that of a centered dipole (moment = 0.21 gauss-*R_S^3*; where one Saturn radius,* R_S*, is 60,330 kilometers) tilted approximately 0.8° from the rotation axis. Near closest approach to Saturn, Voyager 2 traversed a kronographic longitude and latitude range that was complementary to that of Voyager 1. Somewhat surprisingly, no evidence was found in the data or the analysis for any large-scale magnetic anomaly in the northern hemisphere which could be associated with the periodic modulation of Saturnian kilometric radiation radio emissions. Voyager 2 crossed the magnetopause of a relatively compressed Saturnian magnetosphere at 18.5* R_S *while inbound near the noon meridian. Outbound, near the dawn meridian, the magnetosphere had expanded considerably and the magnetopause boundary was not observed until the spacecraft reached 48.4 to 50.9* R_S *and possibly beyond. Throughout the outbound magnetosphere passage, a period of 46 hours (4.5 Saturn rotations), the field was relatively steady and smooth showing no evidence for any azimuthal asymmetry or magnetic anomaly in the planetary field. We are thus left with a rather enigmatic situation to understand the basic source of Saturnian kilometric radiation modulation, other than the small dipole tilt.*

In this report we present results of a study of the magnetosphere and planetary magnetic field of Saturn as observed by Voyager 2. The magnetometers (*1*) operated normally throughout the encounter. The instrumentation of the Voyager 2 magnetic field experiment is identical to that on Voyager 1 (*2*) with the instrument automatically changing ranges as required by the measured field. The minimum quantization step size of $\pm$ 0.0044 nanotesla (nT) in the lowest range of $\pm$ 8.8 nT full scale increased to $\pm$ 0.51 nT in the $\pm$ 2100 nT range near closest approach. As before (*2*), vector measurements at 60-msec intervals were averaged over 1.92, 9.6, and 48 seconds, 16 minutes, and 1 hour.

The maximum measured field intensity of 1187 nT was observed at a kronographic latitude of 17.3°N and longitude (Saturn longitude system, SLS) (*3*) of 322.3°, just before periapsis at 2.69 R_S (1 R_S = 60,330 km). This value was only a few nanoteslas larger than expected, based on a Voyager 1–derived model (*2*) magnetosphere, which had a centered dipole tilted 0.7° with magnetic moment 0.21 gauss-R_S^3 and an azimuthal equatorial ring current (*4*) of 7×10^6 A to represent the magnetic field for $R < 15$ R_S. The spacecraft crossed the equatorial plane only once, at 2.87 R_S just after closest approach. There were no special close encounters with any of the Saturnian satellites, such as were accomplished by Voyager 1 at Titan (*2, 5*), at least from the viewpoint of being within five or fewer satellite diameters.

The main objective for the magnetometer experiment was to determine the location and characteristics of the presumed northern hemisphere magnetic anomaly responsible for the periodic modulation of the Saturnian kilometric radiation (SKR) radio emissions (*6*). Another objective was to compare the magnetic field characteristics of the Saturnian magnetosphere with those observed by Voyager 1 and Pioneer 11.

Bow shock, magnetopause, and magnetosheath. Voyager 2 observed multiple bow shock and magnetopause (MP) crossings during its inbound and outbound trajectory. Figure 1 (right side) shows the trajectory of Voyager 2 in cylindrical coordinates. The axis of symmetry of the system is along the planet-sun line. A filled dot on the trajectory denotes start of a day (for example, 236 is 24 August 1981). For comparison, the Voyager 1 trajectory is shown (left side), also in cylindrical coordinates. The Voyager 1 model bow shock and MP boundaries (*2*) are also displayed. Table 1 gives a preliminary listing of bow shock and MP boundary crossing times and planetocentric radial distances, based on the Voyager 2 magnetometer data. There were multiple crossings of both boundaries: five inbound bow shocks, one inbound MP, at least five well-defined outbound MP's, and seven outbound bow shocks. The average inbound and outbound bow shock crossing positions are shown by line segments intersecting the Voyager 2 trajectory on days 236 and 242, respectively.

The MP of all known magnetospheres is most commonly observed to be a tangential magnetohydrodynamic discontinuity. To accurately estimate the direction normal to that boundary for the MP crossings in Table 1, we used a magnetic field variance method (*7*) well suited for analyzing tangential discontinuities. The analysis to determine the inbound normal yielded an estimate of

$\theta_{in} = 6° \pm 10°$ and $\phi_{in} = 25° \pm 10°$, where θ is the latitude with respect to the sun's equatorial plane, and ϕ is the longitude measured in that plane with $\phi = 0°$ being in the sunward direction. A similar analysis of the five outbound MP crossings yielded an average normal orientation of $\theta_{out} = -18° \pm 5°$ and $\phi_{out} = 57° \pm 7°$. The observed local normals all agree well with values to be expected from the shape of the magnetopause.

When the Voyager 2 boundary crossing distances (Table 1) are compared to those of Voyager 1 at Saturn (*2*), it is apparent that during the Voyager 2 encounter external solar wind conditions must have changed significantly from the time of the inbound MP crossing to that of the outbound crossings (a time interval of 3 days, 10 hours, which is about eight Saturn rotations). Therefore, two model MP boundaries, assumed to be geometrically similar in shape, were derived for the two cases, inbound, 1, and outbound, 2. That is, the MP boundaries were assumed to be paraboloids of revolution about the X axis such that $X_2 = \alpha X_1$ and $\rho_2 = \alpha\rho_1$ (the similarity condition) where

$$(\rho_i/r°_i)^2 = (a_i/r°_i)(1 - X_i/r°_i) \quad (i = 1,2)$$

$r°_{1,2}$ being the planetocentric MP subsolar point distance for the two cases, and $\rho_i = (Y_i^2 + Z_i^2)^{1/2}$. Under the similarity condition, it is easily shown that $a_i/r°_i$ is a constant. Using the average crossing positions and the reasonably well determined longitude of the outbound normal ($\phi_2 = 57°$; predicted to be 70° based on the Voyager 1 model MP), one can determine the four quantities $a_{1,2}$ and $r°_{1,2}$. They were: $a_1 = 37$, $a_2 = 64$, $r°_1 = 19$, and $r°_2 = 32$, all in R_S units. The Voyager 2 inbound and outbound model MP boundaries are also shown in Fig. 1 (right side). Obtaining the slope of the curve at the point of the spacecraft inbound crossing yielded ϕ_1 (model) = 20°, in good agreement with the observed $\phi_1 = 25° \pm 10°$. The ratio of MP subsolar point distances was $r°_2/r°_1 = \alpha = 1.7$. If it can be assumed that these distances can be related to the solar wind ram pressure by the 1/6 power law (*8*), then this ratio implies that the pressure decreased by a factor of $\sim (1.7)^6 = 24$ between inbound and outbound crossings. However, this estimate has a large associated uncertainty, since $r°_2 = 32\ R_S$ may be uncertain by as much as $\pm 5\ R_S$ (but the value $r°_1 = 19\ R_S$ is well determined), and the power of six significantly magnifies the error in the computed ram pressure ratio.

Figure 2 gives an overview of the Voyager 2 encounter in terms of the measured field magnitude (16-minute averages) and associated root-mean-square (RMS). The asymmetry and the maximum field (1187 nT) is due to both a latitude effect and the choice of trajectory with respect to planetary local time. The range and numbers of bow shock and MP crossings are noted at the top of the figure. There were at least five outbound MP crossings, and the range over which they occur may be extended after further study. The increase in RMS as B_{max} is approached is due to the spatial gradient of the field and not to temporal variations, as is the case for the enhanced RMS's in the far magnetosphere and magnetosheath.

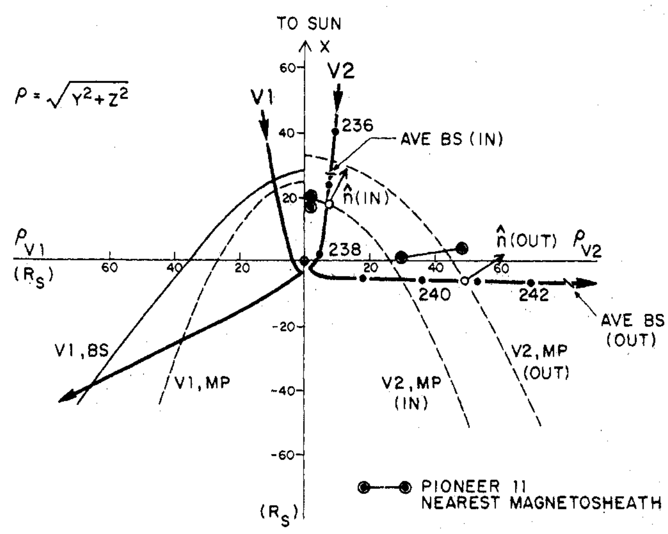

Fig. 1. The trajectories of Voyager 1 (*V1*) (left side) and Voyager 2 (*V2*) (right side) in cylindrical coordinates where X is positive toward the sun and X, Y, Z are orthogonal. Model bow shock (*BS*) and magnetopause (*MP*) boundaries are given (see text). Distance units are in Saturn radii, R_S. Pioneer 11 "nearest magnetosheath" refers to that portion lying between the nearest observed MP and the nearest observed bow shock for inbound and outbound traversals (*17*).

Outer magnetosphere. The average magnetic field geometry observed by Voyager 2 in the Saturnian magnetosphere is shown in Figs. 3 and 4. Given are the hourly averaged X-Y (Fig. 3a), Y-Z (Fig. 3b), and X-Z (Fig. 4) vector component projections along the trajectory. The coordinates are planetocentric solar magnetospheric (SM), with X_{SM} toward the sun, Z_{SM} positive northward and oriented such that the planetary dipole axis lies in the X_{SM}-Z_{SM} plane. The magnetic dipole axis was assumed to be perfectly aligned with the rotation axis, and so the SM coordinates are, in this case, a fixed-orientation system. Also shown are the two cylindrically symmetric inbound and outbound magnetopause surfaces already described. The large-scale structure of the outer magnetosphere of Saturn is illustrated by these vector data, which begin on 237/0700 at a radial distance of 18 R_S and end with 240/1300 at a radial distance of 46 R_S.

Table 1. Saturn's bow shock (BS) and magnetopause (MP) boundary crossings observed by Voyager 2.

Type of crossing	Day	Center time (UT)	Distance (R_S)
	Inbound		
BS	236	1337	31.5
BS	236	1709	29.6
BS	236	1830	27.9
BS	236	2021	26.7
BS	237	0026	23.5
MP	237	0700	18.5
	Outbound		
MP	240	1647	48.4
MP	240	1743	49.0
MP	240	1813	49.4
MP	240	1828	49.6
MP	240	2037	50.9
BS	242	1041	77.3
BS	242	1123	77.7
BS	242	1125	77.8
BS	242	1405	79.6
BS	242	1946	83.4
BS	243	0003	86.2
BS	243	0109	87.0

Inbound at hour 7, when Voyager 2 was above the equatorial plane, the field was predominantly southward (−6.6 nT), but also had substantial sunward (2.5 nT) and eastward (1.8 nT) components. This orientation persisted until hour 10, when the field began rotating toward the radial direction with a reduction in the relative size of the eastward component and a corresponding increase in the sunward component to a value comparable with the southward component.

After passing through the mainly dipolar region of the inner magnetosphere, Voyager 2 followed an outbound trajectory which nearly paralleled the dawn meridian plane at a relatively high southern latitude (30°S). The hourly data show that throughout this region the magnetic field was uniform, with little variation in magnitude and direction other than grad-

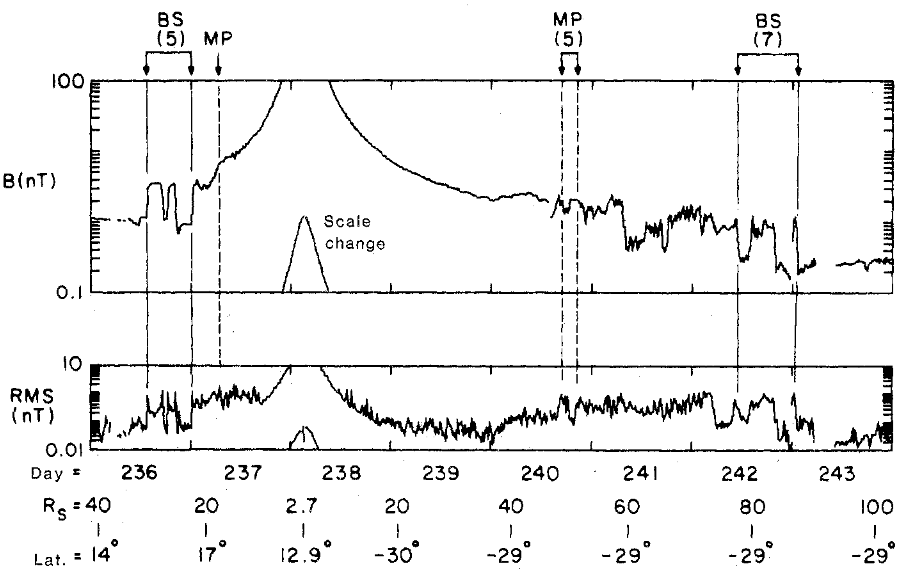

Fig. 2. An overview of the magnitude (B) and Pythagorean mean RMS of the magnetic field measured by Voyager 2 for 8 days around closest approach to Saturn. Shown are 16-minute averages; R_S is the planetocentric radial distance of Voyager 2 and *Lat.* is the latitude of Voyager 2 with respect to Saturn's equatorial plane.

ual changes with increasing distance. Beyond 15 R_S the field remained approximately parallel to the equatorial plane until near the outbound MP, where it became variable for the first time and showed a small southward component (Fig. 4). Throughout this region the field direction was consistent with a sweeping back of the magnetic field out of meridian planes to form the southern lobe of Saturn's magnetotail.

Because of the high kronographic latitude at which the spacecraft traversed the magnetosphere outbound, no tail current sheet crossings were observed by Voyager 2. There was a similar absence of current sheet traversals in the Voyager 1 observations (*2*), whereas Pioneer 11 (*9*) detected field polarity reversals while outbound near the dawn terminator at near equatorial latitudes.

From the first observed outbound MP position it is estimated that the enlarged magnetosphere had a tail diameter of at least 100 R_S, compared with an estimated diameter of 80 R_S at the time of the Voyager 1 encounter. Direct measurements of the fully developed magnetic tail field during the Voyager 2 outbound pass were not made because the spacecraft did not enter the fully developed tail lobe as did Voyager 1.

Comparison of the Voyager 2 outer magnetosphere measurements with those obtained by Voyager 1 provides information about the temporal variation of the Saturnian magnetosphere during the two encounters. First, the magnetic field observed outbound ($R > 15\ R_S$) on Voyager 2 over a period of 46 hours, equal to 4.5 Saturn rotations, was very smooth in character, in contrast to the changes seen in the northern tail lobe field by Voyager 1. This is consistent with the previous interpretations in that the changes observed by Voyager 1 were temporal variations caused by changes in the solar wind (*2, 10*). No evidence of any variation of the field which can be associated with the rotation of the planet was observed by Voyager 2. Hence there is no evidence in these data for any

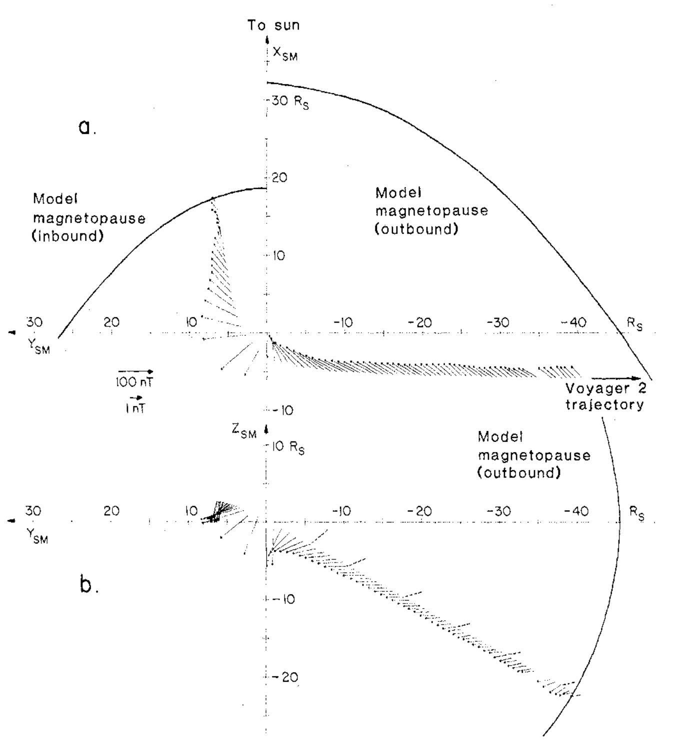

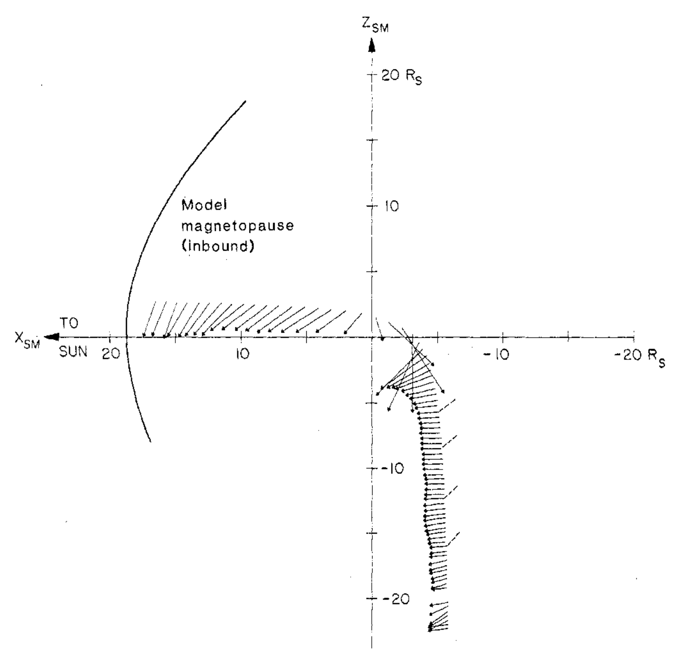

Fig. 3 (left). Projection of hourly average magnetic field components in the Saturnian magnetosphere onto the solar magnetospheric (*SM*) *X-Y* (a) and *Y-Z* (b) planes along the Voyager 2 trajectory. A logarithmic scale has been used to represent field magnitude. Dashed line segments at selected points along trajectory in (b) indicate projected orientation of undistorted dipole field at that position for a planetary magnetic dipole of moment 0.21 gauss R_S^3. Fig. 4 (right). Projection of hourly average magnetic field components onto the solar magnetospheric *X-Z* plane. Dashed line segments indicate projected orientation of undistorted dipole field (see legend to Fig. 3).

asymmetry of the magnetosphere or large-scale anomaly associated with the modulation of the SKR emissions (6).

A comparison of the Voyager 1 and Voyager 2 inbound data, together with the conditions already discussed, indicates that the change in the solar wind conditions responsible for the expansion of Saturn's magnetosphere (evidenced by the observed MP boundaries) occurred during the inbound part of the Voyager 2 encounter. Specifically, the inbound observations for Voyager 1 showed a field that near the equatorial region was almost totally southward in the outermost part of the dayside magnetosphere (2), varying smoothly and in a manner expected for a predominantly compressed dipolar field with an axially symmetric ring current as the inner magnetosphere was approached. The Voyager 2 hourly averages inbound show that the field was deformed in a way consistent with more boundary compression than observed by Voyager 1, that is, it was rotated toward the east relative to an undistorted meridian plane orientation at that longitude.

The 6-hour interval (day 237, hours 1000 to 1600) during which the field orientation rotated toward the sun is considered to be a result of the dynamic response of Saturn's magnetosphere to a sudden decrease in solar wind ram pressure. The field became more nearly radial in direction, suggesting a relaxation of the magnetosphere as the sunward boundry moved to a more distant location. Indeed, the similarity between this field disturbance and the ~ 6-hour disturbance observed by Voyager 1 outbound [seen most clearly in figure 4b of Ness *et al.* (2)] suggests that approximately 6 hours is a characteristic response time of Saturn's magnetosphere to sudden changes in the solar wind ram pressure. This is consistent with propagation of a disturbance at ~ 400 km/sec over a length of ~ 150 R_S, taken to be a characteristic length of Saturn's magnetotail. The smooth character of the average field for the remainder of the encounter, together with the extreme distance of the outbound magnetopause, suggests that the magnetosphere remained expanded at least until the spacecraft was no longer inside it.

Inner magnetosphere and intrinsic planetary field. The Voyager 2 trajectory, although constrained primarily by the Uranus 1986 encounter, nonetheless provided a good opportunity to sample relatively high latitudes in both hemispheres, and the first close-in observations in the northern hemisphere. The close encounter trajectories of Pioneer 11, Voyager 1, and Voyager 2 are illustrated in a kronographic coordinate system in Fig. 5, emphasizing the longitudinal coverage of the near-planet observations of each flyby. Voyager 2 approached Saturn from the northern hemisphere, reaching 29.5°N latitude at a radial distance of 4.0 R_S, well before the closest approach of 2.69 R_S at 12.8°N. Voyager 2 crossed the ring plane at 2.87 R_S and continued southward, approaching 30°S latitude. In contrast, Voyager 1 had remained in the southern hemisphere throughout most of the near encounter period ($R < 10\ R_S$), whereas Pioneer 11 remained within ~ 6° of Saturn's equatorial plane throughout its encounter. Also illustrated in Fig. 5 is the complementary longitudinal extent of the Voyager 2 trajectory near periapsis, which occurred at 323° in Saturn's longitude system, diametrically opposite from the closest approaches of both Pioneer 11 and Voyager 1. This aspect of the Voyager 2 encounter trajectory may prove helpful in separating contributions to the magnetic field observations which are associated directly with Saturn from those fixed in local time (for example, current systems driven by solar wind and solar radiation asymmetries).

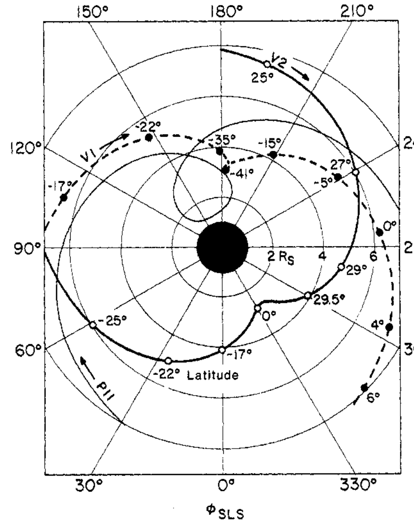

Fig. 5. Presentation of trajectories of Pioneer 11 (*P11*), Voyager 1 (*V1*), and Voyager 2 (*V2*) in a quasi-cylindrical kronographic coordinate system. The radial distance from the planet is shown at the correct longitude in the traditional SLS system. Latitudes of Voyager 1 and Voyager 2 are shown at several points along those trajectories.

The maximum field measured by Voyager 2 was 1187 nT at day 238, hour 0304, approximately 30 minutes prior to nearest approach, within a few nanoteslas of that predicted for a centered, aligned dipole of moment 0.21 gauss-$R_S{}^3$ or the ~ 1° tilted dipole model obtained from Voyager 1 observations (2, 11) but ~ 50 nT greater than that expected of a 0.2 gauss-$R_S{}^3$ dipole, offset to the north by 0.04 R_S (9).

The preliminary spacecraft (and sensor) attitude and engineering data do not allow an improved determination of Saturn's intrinsic planetary field. From an analysis of vector magnetometer data near closest approach, during a spacecraft roll maneuver (FSMAN 4) at day 238, hour 0309, we conclude that a spacecraft orientation error of ~ 1° exists in the SEDR (supplementary experiment data record) now available. Since this roll maneuver directly precedes the sequence of narrow angle camera images which failed to target properly, we conclude that the roll maneuver was not properly executed and that the spacecraft orientation following this roll was in error by ~ 1°.

Saturn's main field is mainly dipolar with an axis nearly aligned with the

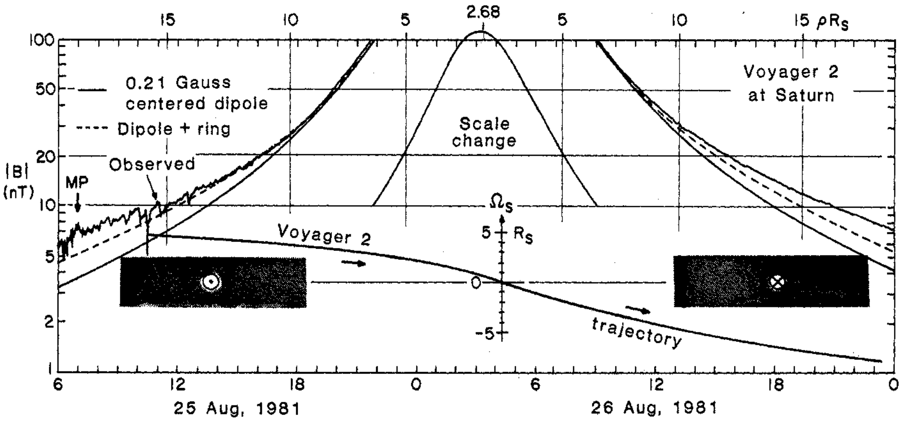

Fig. 6. Comparison of the magnitude of the magnetic field observed by Voyager 2 with pure dipole and dipole plus ring current models. The Voyager 2 trajectory is illustrated beneath the observations showing distance from the equatorial plane as a function of time. Note the different scale used for vertical distance of the spacecraft position.

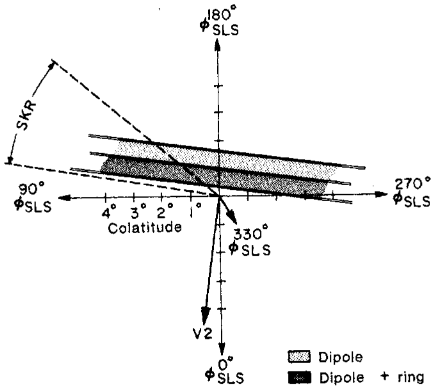

Fig. 7. Interrelationship of postulated dipole tilt angle and SLS phase to account for microabsorption feature at Tethys. The SLS longitude of Voyager 2 at the microabsorption event time is indicated (*V2*) as well as preferred longitude of SKR emissions. The ϕ_{SLS} = 330° is the dipole tilt longitude derived from the Voyager 1 study (*11*).

rotation axis. The sensitivity of derived spherical harmonic magnetic field models to small correlated errors present in flyby observations precludes any attempt to improve substantially on the Voyager 1 models (*11*) until a careful analysis of engineering data can be completed. At present, however, we can confidently utilize the Voyager 2 observed field magnitudes, because they are insensitive to orientation errors (and disturbances perpendicular to Saturn's field, for example, field-aligned current signatures). The use of field magnitudes rather than the vector observations thus results in a considerable loss of information content and a correspondingly greater nonuniqueness in field models derived from the observations, but is mandated by the need for accurate and unbiased observations.

We have therefore chosen to combine the Voyager 1 vector observations and the Voyager 2 magnitude observations obtained within 8 R_S and to perform a nonlinear least-squares inversion (*12*) to obtain a best fitting I1E1 (one internal, one external order) spherical harmonic model. That model has the following Schmidt normalized spherical harmonic coefficients: $g_1^0 = 0.21110$ gauss, $g_1^1 = 0.00072$ gauss, $h_1^1 = 0.00288$ gauss; external, $G_1^0 = -12$ nT, $G_1^1 = 1$ nT, $H_1^1 = -3$ nT, yielding a dipole tilt of 0.81° toward an SLS longitude of 284°. This model has an associated weighted RMS difference of 4.3 nT between the model field and the combined Voyager 1 vector observations and Voyager 2 magnitude observations. Further improvements in models of Saturn's planetary magnetic field can be expected as improved spacecraft attitude and engineering data become available.

Figure 6 displays the magnitude of the observed field compared with that of a centered dipole (moment: 0.21 gauss-R_S^3) with (dashed line) and without (solid line) a contribution from an equatorial ring current. The dashed line corresponds to the model magnetosphere inferred from the Voyager 1 observations (*4*) in which $\sim 7 \times 10^6$ A current flows in a ring 5 R_S thick, extending from 8.5 to 15.5 R_S in Saturn's equatorial plane. The model ring current leads to an enhanced field magnitude along most of the Voyager 2 encounter trajectory, a consequence of the relatively high latitude of Voyager 2 and the solenoidal geometry of the field of the ring current. The agreement between the Voyager 2 observed field magnitudes and the Voyager 1 model is quite good along the inbound trajectory on day 237, except in the vicinity of the inbound magnetopause where local magnetopause surface currents (not modeled) contribute to the observed field. Outbound, on 26 August, the Voyager 2 observed field magnitudes are considerably greater at radial distances in excess of 10 R_S than predicted on the basis of the Voyager 1 model magnetosphere.

Although a detailed study of fields originating external to Saturn is not yet possible, we can offer some insight of a general nature into the lack of agreement. The lack of agreement may be due to either (i) a temporal effect of variations in the solar wind momentum flux, in which the expansion of Saturn's magnetosphere, inferred from the inbound and outbound MP observations, may have contributed to an enhanced ring current during the Voyager 2 outbound pass, or (ii) the neglect in this model of the magnetotail currents associated with the solar wind interaction (*10*). The asymmetries introduced by the solar wind interaction were apparent in the Voyager 1 observations at distances > 15 R_S. These asymmetries were also strongly evident along the Voyager 2 outbound trajectory, near the dawn meridian, as shown in Figs. 3 and 4 and discussed in the preceding section.

Microabsorption features of radiation belt observations. Saturn's ring current has important implications for charged particle motion in Saturn's magnetosphere, particularly for the absorption of trapped radiation by its many satellites and rings. Observations of charged particles, confined to motion along field lines and drift shells, can be useful in the determination of field line geometry; indeed, the Voyager 1 observation (*13*) of a microabsorption feature, attributed to the satellite Rhea, provided an independent and conclusive test of the magnetic

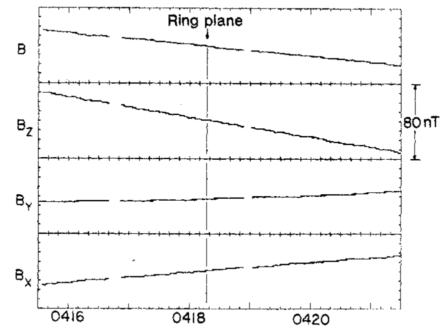

Fig. 8. Detailed 60-msec samples of vector magnetic field as observed during ± 3 minutes centered at ring plane crossing. Individual orthogonal sensor components B_x, B_y, and B_z (in spacecraft coordinates) are presented as well as B, the scalar magnitude (see text).

field geometry derived from the Voyager 1 model magnetosphere (*4*).

A similar microabsorption feature observed by the cosmic-ray experiment in Voyager 2 (*14*) near the L shell of Tethys may ultimately yield an important constraint on internal field models (for example, phase of the dipole tilt). Factors influencing the field line geometry between Tethys, near Saturn's equator, and Voyager 2 at ~ 20°S latitude, which must be considered in modeling the microabsorption feature include: (i) Saturn's dipole tilt, (ii) a possible polar or equatorial offset of the dipole, and (iii) the radial stretching of field lines near Saturn's equatorial plane due to the ring current. A single absorption feature, even with the simplest of assumptions, leads not to a unique solution of a dipole tilt but rather to a range of permissible combinations of dipole tilts and longitudinal phases. In a dipole field, a change in the L parameter (ΔL) is simply related to a change in the magnetic latitude (λ) by $\Delta L/L = 2 \tan \lambda \, \Delta\lambda$. A small $\Delta\lambda$ observed at a longitudinal phase ϕ is likewise simply related to the tilt (θ_0) and phase (ϕ_0) of the dipole by $\Delta\lambda = -\theta_0 \cos(\phi - \phi_0)$ for small tilts and $\Delta\lambda$. Thus, a single observation ΔL (equivalently $\Delta\lambda$) determines only the product of θ_0 and $\cos(\phi - \phi_0)$. The present lack of accurate engineering and ephemeris information precludes a detailed analysis, but in Fig. 7 we illustrate the basic features of such a solution and the relative magnitudes of several important parameters in the analysis appropriate to the Saturn situation.

Each band in Fig. 7 extending perpendicular to the spacecraft position vector (7.5° SLS) at the microabsorption event time of day 238, hour 0630 represents the range of dipole tilts and phases for which Voyager 2 and Tethys share the same "L shell." The width of each band corresponds to an uncertainty of a satellite diameter in radial position, the upper band determined by considering a dipole tilt only while the lower band represents possible dipole tilt solutions when the effects of Saturn's ring current are considered. For the latter solution, field lines must be traced numerically from Voyager 2 to the equator. The Voyager 1 model of Saturn's ring current has been assumed in this example for demonstration purposes, although it is clear from the preceding discussion that the ring current and hence the nondipolar character of the field geometry may have been significantly changed at the time Voyager 2 encountered the Tethys L shell outbound. Both solutions demonstrate insensitivity to a rotation of the dipole tilt about the Saturn-spacecraft vector (or a translation of the dipole perpendicular to the Saturn-spacecraft vector).

Additional constraints based on particle species identification, the relative longitude of Tethys and Voyager 2 at event time, and particle drifts due to field gradients and curvature may further constrain the range of possible solutions. Clearly additional microabsorption features at longitudes around 90° or 270° SLS would also further constrain the solution.

Ring plane crossing. Because of the special circumstances (*15*, *16*) surrounding the crossing of the ring plane by Voyager 2, we have investigated the detailed 60-msec data during a 16-minute interval centered on the nominal crossing time at day 238, hour 0418, for evidence of any unusual anomalies, and the central 6 minutes of these data are plotted in Fig. 8. There are no sudden changes evident or quasi-periodic variations that could be associated with any mechanical motion of the magnetometer sensor or with any localized field perturbations or wave phenomena. The regular toggling of the individual components between adjacent digital values is readily evident because the magnetic field components changed gradually throughout this sample. Note the very expanded scale of the plots in this figure, where the field intensity is approximately 1100 nT, so that the quantization step size of the 12-bit A-D converter yields a ± 0.5-nT uncertainty. This is well above the intrinsic noise level of the sensors measured in flight, which is less than 0.006 nT RMS equivalent over the 8.3-Hz bandwidth.

We conclude that there is no evidence in these detailed data for any special event or events which would have disturbed either the assumed orientation of magnetometer sensors or the ambient field at the location. The sensitivity is limited only by the quantization step size and the vector sample rate of $16\frac{2}{3}$/second (Nyquist frequency = 8.33 Hz). The quantization limitation translates to an insensitivity to angular variations of less than 1.5 arc minutes. Short time scale events manifested as magnetic disturbances would be progressively attenuated by the instrument frequency roll-off characteristics beyond 5 Hz.

NORMAN F. NESS
MARIO H. ACUÑA
KENNETH W. BEHANNON
LEONARD F. BURLAGA
JOHN E. P. CONNERNEY
RONALD P. LEPPING
Laboratory for Extraterrestrial Physics, Goddard Space Flight Center, Greenbelt, Maryland 20771
FRITZ M. NEUBAUER
Technische Universität, Braunschweig, Federal Republic of Germany

References and Notes

1. K. W. Behannon, M. H. Acuña, L. F. Burlaga, R. P. Lepping, N. F. Ness, F. M. Neubauer, *Space Sci. Rev.* **21**, 235 (1977).
2. N. F. Ness, M. H. Acuña, R. P. Lepping, J. E. P. Connerney, K. W. Behannon, L. F. Burlaga, F. M. Neubauer, *Science* **212**, 211 (1981).
3. M. D. Desch and M. L. Kaiser, *Geophys. Res. Lett.* **8**, 253 (1981).
4. J. E. P. Connerney, M. H. Acuña, N. F. Ness, *Nature (London)* **292**, 724 (1981). The total current in the Voyager 1 model ring is ~ 7 × 10^6 A but was incorrectly given in this reference as 3 × 10^6.
5. N. F. Ness, M. H. Acuña, K. W. Behannon, F. M. Neubauer, *J. Geophys. Res.*, in press.
6. M. L. Kaiser *et al.*, *Nature (London)* **292**, 731 (1981).
7. G. L. Siscoe, L. Davis, Jr., P. J. Coleman, Jr., E. J. Smith, D. E. Jones, *ibid.* **73**, 61 (1968).
8. J. Y. Choe, D. B. Beard, E. C. Sullivan, *Planet. Space Sci.* **21**, 485 (1973).
9. E. J. Smith, L. Davis, Jr., D. E. Jones, P. J. Coleman, Jr., D. S. Colburn, P. Dyal, C. P. Sonett, *J. Geophys. Res.* **85**, 5655 (1980).
10. K. W. Behannon, J. E. P. Connerney, N. F. Ness, *Nature (London)* **292**, 753 (1981).
11. M. H. Acuña, J. E. P. Connerney, N. F. Ness, *ibid.*, p. 721.
12. J. E. P. Connerney, *J. Geophys. Res.* **86**, 7679 (1981).
13. R. E. Vogt, D. L. Chenette, A. C. Cummings, T. L. Garrard, E. C. Stone, A. W. Schardt, J. H. Trainor, N. Lal, F. B. McDonald, *Science* **212**, 231 (1981).
14. R. E. Vogt *et al.*, *ibid.* **215**, 577 (1982).
15. J. W. Warwick *et al.*, *ibid.*, p. 583.
16. F. L. Scarf, D. A. Gurnett, W. S. Kurth, R. L. Poynter, *ibid.*, p. 587.
17. J. H. Wolfe, J. D. Mihalov, H. R. Collard, D. D. McKibbin, L. A. Frank, D. S. Intriligator, *ibid.* **207**, 403 (1980).
18. We acknowledge useful discussions of these results with our Voyager colleagues and appreciate the expert assistance of our fellow Laboratory of Experimental Physics computer support staff under the able guidance of W. H. Mish. Finally, the attention given to supporting our experiment by the Jet Propulsion Laboratory staff is recognized and greatly appreciated. One of us, F.M.N., was supported financially by the German Ministry of Science and Technology.

10 November 1981

Plasma Observations Near Saturn: Initial Results from Voyager 2

Abstract. *Results of measurements of plasma electrons and positive ions made during the Voyager 2 encounter with Saturn have been combined with measurements from Voyager 1 and Pioneer 11 to define more clearly the configuration of plasma in the Saturnian magnetosphere. The general morphology is well represented by four regions: (i) the shocked solar wind plasma in the magnetosheath, observed between about 30 and 22 Saturn radii* (R_S) *near the noon meridian; (ii) a variable density region between* ~ *17* R_S *and the magnetopause; (iii) an extended thick plasma sheet between* ~ *17 and* ~ *7* R_S *symmetrical with respect to Saturn's equatorial plane and rotation axis; and (iv) an inner plasma torus that probably originates from local sources and extends inward from* $L \approx 7$ *to less than* $L \approx 2.7$ (L *is the magnetic shell parameter). In general, the heavy ions, probably* O^+, *are more closely confined to the equatorial plane than* H^+, *so that the ratio of heavy to light ions varies along the trajectory according to the distance of the spacecraft from the equatorial plane. The general configuration of the plasma sheet at Saturn found by Voyager 1 is confirmed, with some notable differences and additions. The "extended plasma sheet," observed between* $L \approx 7$ *and* $L \approx 15$ *by Voyager 1 is considerably thicker as observed by Voyager 2. Inward of* $L \approx 4$, *the plasma sheet collapses to a thin region about the equatorial plane. At the ring plane crossing,* $L \approx 2.7$, *the observations are consistent with a density of* O^+ *of* ~ *100 per cubic centimeter, with a temperature of* ~ *10 electron volts. The location of the bow shock and magnetopause crossings were consistent with those previously observed. The entire magnetosphere was larger during the outbound passage of Voyager 2 than had been previously observed; however, a magnetosphere of this size or larger is expected* ~ *3 percent of the time.*

Before the Voyager 2 encounter with Saturn, our knowledge of the Saturnian magnetosphere was based on the results of the Pioneer 11 (*1*) and Voyager 1 (*2*) flybys. Since the inbound trajectories of Pioneer 11 and Voyager 1 were close to the noon meridian and to the equatorial plane of Saturn, measurements could be made only for a limited range of latitudes. The Voyager 2 trajectory tra-

0036-8075/82/0129-0563$01.00/0